Published in final edited form as:
*Curr Protoc Cytom*. 2011 October ; CHAPTER: Unit9.37. doi:10.1002/0471142956.cy0937s58.

# Assessing Mitochondrial Redox Status by Flow Cytometric Methods: Vascular Response to Fluid Shear Stress

**Rongsong Li**, **Nelson Jen**, **Fei Yu**, and **Tzung K. Hsiai**
Cardiovascular Engineering Research, Department of Biomedical Engineering and Cardiology, School of Medicine and School of Engineering, University of Southern California, Los Angeles, California

## Abstract

Mitochondria are an important source of superoxide production contributing to physiological and pathological responses, including vascular oxidative stress that is relevant to cardiovascular diseases. Vascular oxidative stress is intimately linked with pro-inflammatory states and atherosclerosis. Oxidized low density lipoprotein (OxLDL) modulates intracellular redox status and induces apoptosis in endothelial cells. Hemodynamic, specifically, fluid shear stress imparts both biomechanical and metabolic effects on vasculature. Mitochondria are an important source of superoxide production contributing to vascular oxidative stress with relevance to cardiovascular diseases. We hereby present biophysical and biochemical approaches, including fluorescence-activate cell sorting, to assess the dynamics of vascular redox status

### Keywords

Flow cytometry; oxidative stress; shear stress; mitochondrial redox status

## INTRODUCTION

Growing evidence supports the role of reactive oxygen and nitrogen species in the etiology of atherosclerosis. The manifestations of atherosclerosis tend to be focal and eccentric (Harrison, Griendling et al. 2003; Sorescu, Song et al. 2004; Hsiai, Hwang et al. 2007). Vascular oxidative stress and pro-inflammatory states mediate endothelial cell homeostasis with relevance to the initiation of atherosclerosis. Low-density lipoprotein (LDL), a major risk factor of atherosclerosis, transmigrates across the vascular wall to the subendothelial layer in which it undergoes oxidative modifications (Navab, Berliner et al. 1996; Stocker and Keaney Jr 2004). Oxidized LDL (OxLDL) mediates endothelial redox status (Cominacini, Pasini et al. 2002) and apoptosis at a high concentration (Dimmeler, Haendeler et al. 1997; Harada-Shiba, Kinoshita et al. 1998; Martinet and Kockx 2001). Hemodynamic, namely, fluid shear forces, regulates the generation of reactive nitrogen species (RNS) and reactive oxygen species (ROS)(Hwang, Ing et al. 2003; Hwang, Saha et al. 2003; Hsiai, Hwang et al. 2007). While endothelial nitric oxide synthase (eNOS) is the major source of reactive nitrogen species (RNS), NADPH oxidase is considered a major source of ROS in vascular endothelial cells (Gorlach, Brandes et al. 2000; Hsiai, Hwang et al. 2007). Mitochondria are also an important source of cellular superoxide anion ($O_2^{\cdot -}$) and hydrogen peroxide ($H_2O_2$) (Griendling and FitzGerald 2003). In particular, OxLDL induces mitochondrial superoxide ($mtO_2^{\cdot -}$) production (Zmijewski, Moellering et al. 2005; Gutierrez, Ballinger et al. 2006; Davidson and Duchen 2007) and apoptosis in vascular cells, including endothelial cells (de Nigris, Franconi et al. 2000; Li, Wang et al. 2006; Cheng, Cui et al. 2007; Deng, Zhang et al. 2009; Liu, Zhao et al. 2009). Our study has demonstrated that fluid shear stress also modulated mitochondrial superoxide production.

In the mitochondria, oxidative phosphorylation from complexes I to II, III and IV drives the proton translocation across the inner membrane to the intermembrane space (Duchen, Surin et al. 2003). The proton gradient is expressed as mitochondrial membrane potential ($\Delta\Psi_m$) (Chen 1988); this gradient drives the production of ATP by complex V, ATP synthetase. The transfer of of electrons from ubisemiquinone through the mitochondrial respiratory chain more than 98% efficient, however, 1.5 to 2 % of electrons leak out to form superoxide anion ($O_2^{\cdot -}$) mainly at complex I (NADH coenzymeQ reductase) and III (ubiquinol cytochrome *c* reductase) (Forman 1999). The superoxide anion is converted to $H_2O_2$ in mitochondria by superoxide dismutase.

The application of flow cytometry or fluorescence-activate cell sorting (FACS) has enabled a quantitative approach to assess mitochondrial redox status in terms of $\Delta\Psi_m$ and $mtO_2^{\cdot -}$production. In this chapter, we will address the methodology to assess the dynamics of mitochondrial redox status and vascular oxidative stress in response to fluid shear stress.

## BASIC PROTOCOL

### ASSESSING MITOHCONDRRIAL REDOX STATUS IN RESPONSE TO FLUID SHEAR STRESS

Mitochondrial function is relevant to metabolic homeostasis (Nisoli, Clementi et al. 2007).$\Delta\Psi_m$ is an important indicator of mitochondrial energetic state and cell viability (Chen 1988). $\Delta\Psi_m$ is coupled with oxidative phosphorylation to drive ATP synthesis (Liberman, Topaly et al. 1969; Senior 1988). During myocardial reperfusion injury, opening of the mitochondrial permeability transition pore (MPTP) collapses $\Delta\Psi_m$ and uncouples oxidative phosphorylation, resulting in ATP depletion and apoptosis (Beltran, Mathur et al. 2000; Hausenloy and Yellon 2003). Fluid shear stress is reported to influence mitochondrial ATP synthesis, which is coupled with $\Delta\Psi_m$ (Mitchell and Thomas 1979; Kudo, Morigaki et al. 2000). The formation of mitochondrial ROS (mtROS) is dependent on $\Delta\Psi_m$ (Korshunov, Skulachev et al. 1997), and mtROS level increases exponentially as $\Delta\Psi_m$ is increased or hyperpolarized above -140 mV (Lee, Bender et al. 2002). In response to oxidative stress, mitochondrial manganese superoxide dismutase (Mn-SOD) is up-regulated (Storz 2007), and dismutates $O_2^{\cdot -}$ anion to $H_2O_2$. In response to laminar shear stress, cytosolic CuZn-SOD expression is up-regulated (Inoue, Ramasamy et al. 1996).

In this protocol, method and experimental design will be provided to demonstrate that (1) pulsatile shear stress (PSS) increased $\Delta\Psi_m$ via up-regulation of Mn-SOD activities, whereas (2) oscillatory shear stress (OSS) increases $mtO_2^{\cdot -}$ production via NADPH Oxidase and c-Jun $NH_2$-terminal kinase (JNK) signaling.

#### Materials

Bovine (BAEC) or human aortic endothelial cells (HAEC)

Glass slides (5 $cm^2$; BD Bioscience)

Collagen Type I (BD Bioscience)

High glucose (4.5 g/l) DMEM (Invitrogen)

Heat-inactivated fetal bovine serum (Hyclone)

100 U/ml L-glutamine-penicillin-streptomycin (Sigma)

JNK inhibitor SP600125 (10μM)

NADPH oxidase inhibitor apocynin (1mM)

Anti-oxidant N-acetyl cysteine (NAC, 5mM)

siRNA target sequence for Bovine JNK1: 5′-CATGGAGCTCATGGATGCAAA-TCTT-3′ (30 nM)

siRNA target sequence for Bovine JNK2: 5′-CATGAAAGAATGTCCTACCTTCTTT-3′. (30 nM)

Lipofectamine RNAiMAX (Invitrogen)

Negative control siRNA (Qiagen)

Cationic fluorescent dye, tetramethylrhodamine methyl ester ($TMRM^+$) (Molecular probes)

Dulbecco's Phosphate Buffered Saline (DPBSInvitrogen)

High performance digital CCD camera (Pixelfly II, Cooke Corporation)

IPlab software (BD bioscience)

Rotenone (Sigma)

Oligomycin (Alexora)

FCCP (Carbonylcyanide-4-(trifluoromethoxy)-phenylhydrazone) (Sigma)

MnTMPyP (Alexora)

Trypsin (Invitrogen)

MitoSOX Red (Invitrogen)

Dulbecco's Phosphate Buffered Saline supplemented with 2% FBS (Hyclone)

2% Paraformaldehyde

Flow cytometer (e.g. BD LSR II, BD Biosciences)

LDL (isolated from blood samples of fasting adults; (Hwang, Ing et al. 2003)

CuSO4 (Sigma)

EDTA (Signma)

0.22μm filter (Fisher Scientific)

## Seed and prepare cells

**1** Seed BAEC or HAEC cells on glass slides at $1.5 \times 10^5$ cells per slide and grow to confluent monolayers in high glucose (4.5 g/l) DMEM supplemented with 10% heat-inactivated fetal bovine serum, 100 U/ml L-glutamine-penicillin-streptomycin for 48 h in 5% CO2 at 37°C.

**2** Starve cells in DMEM with 0.5% FBS overnight to reduce phosphorylative background prior to shear stress exposure.

## Perform dynamic flow inhibitor study or modulation of gene expression with siRNA

**3** For inhibitor studies, pre-treat cells with either JNK inhibitor SP600125 (10μM) for 30 minutes, NADPH oxidase inhibitor apocynin (1mM) for 2 hours or anti-oxidant N-acetyl cysteine (NAC, 5mM) prior to shear stress exposure. For modulating gene expression, BAEC were transfected with 30 nM of siRNA using Lipofectamine RNAiMAX, and negative control siRNA as the scramble

siRNA. siRNA transfected cells were used 48 hours afterward for confirmation of gene knockdown or functional assay.

**4** BAEC or HAEC were exposed to the following conditions: (1) Control at static conditions, (2)PSS at a time-averaged shear stress ($\tau_{ave}$) of 23 dyn.cm$^{-2}$ and temporal gradient ($\partial\tau/\partial t$) of 71 dyn·cm$^{-2}$·s$^{-1}$ or (3) OSS at $\tau_{ave}$= 0.02 and $\partial\tau/\partial t$ at ± 3 dyn·cm$^{-2}$·s$^{-1}$ for indicated time using A dynamic flow channel simulating hemodynamics in arteries (Hsiai, Cho et al. 2001).

After flow exposure, the cells will undergo parallel procedures either to measure mitochondrial membrane potential (Step 5–9) or measure mitochondrial superoxide production (Step 10–14).

### Measure mitochondrial membrane potential ($\Delta\Psi_m$)

**5** To examine $\Delta\psi_m$ in response to mitochondrial respiratory chain inhibitors and uncouplers, confluent monolayers of endothelial cells were treated for 1 hour at 37°C with: (i) 1μM of rotenone to inhibit the electron transfer from Fe-S centers in Complex I to ubiquinone, (ii) 5μg/mL of oligomycin to inhibit ATP synthase, (iii) 1μM of FCCP, a protonophore and potent uncoupler of oxidative phosphorylation, (iv) 10μM Cyclosporine-A, an inhibitor of mitochondrial permeability transition pores, and (v) 50μM MnTMPyP, a Mn-SOD mimic

**6** Following flow exposure or inhibitor treatment, cells were washed and incubate at 37°C with 10 nM of $TMRM^+$ for 30 min in DPBS

**7** After the incubation, cells were washed with PBS and trypsinized off and re-suspended in 0.5ml of DPBS.

**8** $TMRM^+$ was excited at 488nm, and fluorescence emitted at 588 nm was measured with (FL2) channel by FACS using the FACS Caliber system (BD Biosciences, San Jose, CA).

**9** Fluorescence intensity was used to calculate mitochondrial membrane potential as described in the background information section.

### Quantify mitochondrial superoxide production

**10** Following flow exposure, the cells were incubated with MitoSOX Red (3 μM) at 37°C for 10 minutes.

**11** The cells were then collected by trypsinization and washed with DPBS supplemented with 2% FBS.

**12** The cells were then fixed in 2% paraformaldehyde for 10 min and re-suspended in 0.5ml of PBS with 2% FBS.

**13** Using a flow cytometer, MitoSOX Red was excited at 488 nm and fluorescence emission at 575 was measured.

**14** Relative fluorescence intensity was used as measurement of mitochondrial superoxide production.

**Perform statistical analysis—**Experimental data from step 9 or 14 were analyzed and expressed as mean ± SD. Comparisons of multiple groups were analyzed by one-way analysis of variance (ANOVA). Statistical significance for pairwise comparison was determined by using the Tukey test. P-values of $< 0.05$ are considered statistically significant.

# COMMENTARY

## Background Information

A dynamic flow channel is used to implement pulsatile shear stress (PSS) or oscillatory shear stress (OSS) simulating hemodynamics in human carotid arterial bifurcations. OSS is commonly considered to be an inducer of vascular oxidative stress whereas PSS is considered to reduce oxidative stress (Ku, Giddens et al. 1985; De Keulenaer, Chappell et al. 1998).The flow system is designed to generate well-defined flow profiles across the width of the parallel flow chamber at various temporal gradients ($\partial\tau/\partial t$), frequencies, and amplitudes (Hsiai, Cho et al. 2001). Endothelial cells are exposed to the following conditions: (i) Control at static conditions, (ii) PSS at a time-averaged shear stress ($\tau_{ave}$) of 23 dyn·cm$^{-2}$ with a temporal gradient ($\partial\tau/\partial t$) of 71 dyn.cm$^{-2}$·sec$^{-2}$; and (iii) OSS at $\tau_{ave}$= 0.02 and $\partial\tau/\partial t$ at ±3 dyn·cm$^{-2}$·s$^{-1}$.

MitoSOX Red is a fluorgenic dye selective for mitochondrial superoxide in live cells (Robinson, Janes et al. 2006). It localizes into cellular mitochondria and is readily oxidized by superoxide, but not other sources of reactive oxygen or nitrogen species. Mitosox is hexyl triphenylphosphonium conjugated to hydroethidine (HE); while both HE and Mito-SOX can be oxidized by mitochondrial superoxide, only the later can used to detect mitochondrial specific oxidation when excited at selective wavelength(Robinson, Janes et al. 2006).

$TMRM^+$ is a non-invasive cationic fluorescent dye used to quantify changes in mitochondrial membrane potential (Floryk and Houstek 1999; Scaduto and Grotyohann 1999). TMRM+ is a permeable dye that does not bind to cells and accumulates in the negatively charged mitochondria by electrostatic attraction. A shift in fluorescent intensity corresponds to a depolarization event due to a change in the dye's concentration in the mitochondria. Mitochondrial membrane potential ($\Delta\Psi_m$) was established by probing the fluorescent intensity, followed by applying the Nernst equation(Ehrenberg, Farkas et al. 1987):

$$E=E_0-\frac{RT}{nF}\cdot\log\left(\frac{[TMRM^+]_{in}}{[TMRM^+]_{out}}\right)$$

where *R* denotes the universal gas constant, "*T*" the temperature in Kelvin, "*F*" the Faraday constant and "*n*" the number of electrons transferred in the half reaction. $[TMRM^+]_{in}$ denoted $TMRM^+$ concentration inside and $[TMRM^+]_{out}$ outside the mitochondria. The value of "*RT/nF*" was calculated to be 61mV at 37°C (Cortese 1999; Nicholls 2006). $[TMRM^+]_{out}$ was constant due to the relatively higher concentration than $[TMRM^+]_{in}$, assuming that $E_0$ = $\Delta\Psi_m$ = −140mV at equilibrium under non-stimulation condition(Ehrenberg, Farkas et al. 1987; Loew, Tuft et al. 1993; Nicholls 2006). The changes in $\Delta\Psi_m$ [mV] was determined as follows (Ehrenberg, Farkas et al. 1987; Loew, Tuft et al. 1993; Chacon, Reece et al. 1994; Nicholls 2006):

$$\Delta\Psi m_{stimulation}=-140-61\cdot\log\left(\frac{TMRM^+\mathrm{int}ensity_{stimulation}}{TMRM^+\mathrm{int}ensity_{non-stimulation}}\right)\ [\mathrm{mV}]$$

## Critical Parameters and Troubleshooting

The measurement of mitochondrial redox status in terms of membrane potential and superoxide production with fluorescence dye is a delicate method. Optimization of experimental conditions and performance of a numbers of trials can reduce the inter-

observer variations. The factors that affect the reproducibility include cell conditions, dye concentration, incubation intervals and timing of measurements. The mitochondrial specificity of the fluorescence dye also depends on the concentration of dye and the incubation time with cells. High concentration of dye or prolonged incubation time will likely increase non-specific incorporation of the dyes into other intracellular compartments. Reagents that disrupt membrane potential will also affect the measurement. Cells should be quickly prepared in a dark setting to prevent degradation or shift in fluorescent signals. These issues can be partially alleviated by fixing cells prior to FACS analysis. For superoxide production, MitoSox Red incorporation into mitochondrial relies on mitochondrial membrane potential. Damages to cells may cause mitochondria rupture leading to dye localization to nucleus and non-specific readings. Thus, the metabolic status of the cells constitutes a major confounding variable to the experimental outcomes. Table 9.36.1 provides a list of troubleshooting guides.

## Anticipated Results

**Characterization of $\Delta\psi_m$ in intact endothelial cells—**Mitochondrial respiratory chain inhibitors and uncouplers can be employed to assess the characteristics of $TMRM^+$ dye in intact HAEC (Fig. 9.36.1). Addition of FCCP, a protonophore to uncouple oxidative phosphorylation, will depolarize $\Delta\Psi_m$ in intact cells and decrease the $TMRM^+$ intensity by 25% compared to the control ($P < 0.05$, n=5). Treatment with rotenone, an NADH dehydrogenase inhibitor, will depolarize $\Delta\Psi_m$ and decrease the $TMRM^+$ intensity by 55% ($P < 0.05$, n=5). Treatment with oligomycin, an ATP synthase inhibitor, will hyperpolarize $\Delta\Psi_m$ and increase $TMRM^+$ intensity by 2.5-fold ($P < 0.05$, n=5). Furthermore, cyclosporine-A, an inhibitor of mitochondrial permeability transition pores (MPTP), will increase the $TMRM^+$ intensity by 2.6-fold ($P < 0.05$, n=5). Treatment with FCCP, oligomycin and rotenone will further depolarize $\Delta\Psi_m$ and decrease $TMRM^+$ intensity by 71% ($P < 0.05$, n=5). The changes of $\Delta\Psi_m$ (mV) are in agreement with published results (Cassarino, Swerdlow et al. 1998; Ward, Rego et al. 2000) (Table 9.36.2). Hence, the dynamic range of $TMRM^+$ provides a basis to characterize $\Delta\Psi_m$ in response to shear stress.

**Pulsatile Shear Stress Increases $\Delta\Psi_m$—**While the molecular mechanisms whereby pulsatile versus oscillatory shear stress mediated-$mtO_2^{\cdot-}$ remain to be addressed, we have provided the innovative insights into the dynamics of mitochondrial redox status: (i) Pulsatile shear stress (PSS) increases $\Delta\Psi_m$ in HAEC (Fig. 9.36.2a,b), (ii) PSS up-regulated Mn-SOD mRNA and protein expression (Figs. 9.36.2d–e), and (iii) Mn-SOD up-regulation represents a potential pathway whereby shear stress influenced $\Delta\Psi_m$ (Figs. 9.36.2e) (Li, Beebe et al. 2009).

PSS is considered to be cardioprotective (Hwang, Ing et al. 2003) and our observations suggest that one of the possible mechanisms whereby PSS confers cardioprotection may be due to an increase in $\Delta\Psi_m$ that is important for oxidative phosphorylation and ATP synthesis (Chen 1988).

Although long term PSS reduces oxidative stress, we found that short term exposure of endothelial cells to PSS induced transient mitochondrial superoxide production (Fig. 9.36.3).

**Oscillatory shear stress induced $mtO_2^{\cdot-}$ production via NADPH oxidase and JNK activation—**To examine the mechanisms of shear stress induced mitochondrial superoxide production, we assessed whether NADPH oxidase and JNK activation were implicated. We tested the effects of Apocynin (inhibitor of NADPH Oxidase), JNK inhibitor (SP600125), and JNK knock-down (with JNK siRNA, siJNK) on mitochondrial superoxide

($mtO_2^{\cdot-}$) production in response to OSS. Flow cytometry was employed to quantify MitoSOX Red intensities specific for $mtO_2^{\cdot-}$.

Oscillatory shear stress induced JNK activation (Fig. 9.36.4, Fig. 9.36.6a) and a 2.57-fold increase in mitochondrial superoxide production as compared to the static condition (Fig. 9.36.5). The induction of mitochondrial superoxide by OSS was inhibited by SP600125 (10μM) by 62% (Fig. 9.36.5).

Next, we demonstrated the effect of JNK on $mtO_2^{\cdot-}$ production with siJNK. The knockdown of JNK with siRNA was confirmed by western blot analysis (Fig. 9.36.6c). JNK1 protein level was decreased by 71% and JNK2 by 74% following siJNK transfection. JNK knockdown with siJNK completely inhibited OSS-induced MitoSOX Red intensity as compared to the static condition (Fig. 9.36.6b,d).

Pre-treatment of cells with Apocynin (1mM) also reduced OSS-mediated Mitosox Red intensity from 1.80- to 0.89-fold as compared to the static conditions (Fig. 9.36.7). Taken together, these findings demonstrated the notion that OSS mediated $mtO_2^{\cdot-}$ production via NADPH oxidase and JNK activation.

In corollary, we assessed whether OxLDL induced generation of endothelial $mtO_2^{\cdot-}$ and change in the $\Delta\Psi_m$ via JNK pathway. We silenced JNK1 and JNK2 gene expression with siRNA (siJNK). In response to OxLDL at 50μg/mL for 1 hour, MitoSOX Red intensity was significantly increased by 1.88±0.19-fold (n=3, $P<0.05$) (lane 1 vs. 3) and this increase was reversed by siJNK (88.4% reduced, n=3, $P<0.05$) (lane 3 vs. 6) (Fig. 9.36.8a,b). Similarly, $\Delta\Psi_m$ as converted from the $TMRM^+$ intensity, was significantly increased by 18%, from −149.60±5.64mV to −180.97±0.64mV (n=3, $P<0.05$) (lane 1 vs. 3) in response to OxLDL. This increase was attenuated by siJNK (61.7% reduction, n=3, $P<0.05$), (lane 3 vs. 6) (Fig. 9.36.8c). Native LDL (nLDL) had no effects on $mtO_2^{\cdot-}$ and $\Delta\Psi_m$ (lanes 2 and 5 in Fig. 9.36.8b,c) (n=3, $P>0.05$). Hence, OxLDL-activated JNK influenced mitochondrial redox status.

Overall, we demonstrated that pro-atherogenic factors such as OSS and OxLDL modulate mitochondrial redox status in terms of $mtO_2^{\cdot-}$ production and $\Delta\Psi_m$, which can be quantitatively measured with mitochondrial specific fluorescence dye-based flow cytometry.

### Time considerations

The overall time span for the procedure will be three days for basic protocol and four days if perform gene modulation step. The hands-on time range from 4.5 to 6.5 hours combining all the experimental steps.

## Acknowledgments

The authors would like to express gratitude to the Atherosclerosis Research Unit at UCLA for providing the native and oxidized LDL. These studies were supported by American Heart Association GIA 0655051Y (to T. K. H.) and National Institutes of Health HL-068689 and HL-083015 (to T. K. H.).

## LITERATURE CITED

Beltran B, Mathur A, Duchen MR, Erusalimsky JD, Moncada S. The effect of nitric oxide on cell respiration: A key to understanding its role in cell survival or death. Proceedings of the National Academy of Sciences of the United States of America. 2000; 97(26):14602–14607. [PubMed: 11121062]

Cassarino DS, Swerdlow RH, Parks JK, Parker WD Jr, Bennett JP Jr. Cyclosporin A increases resting mitochondrial membrane potential in SY5Y cells and reverses the depressed mitochondrial

membrane potential of Alzheimer's disease cybrids. Biochemical and Biophysical Research Communications. 1998; 248(1):168–173. [PubMed: 9675105]

Chacon E, Reece JM, Nieminen AL, Zahrebelski G, Herman B, Lemasters JJ. Distribution of electrical potential, pH, free Ca2+, and volume inside cultured adult rabbit cardiac myocytes during chemical hypoxia: a multiparameter digitized confocal microscopic study. Biophysical Journal. 1994; 66(4): 942–952. [PubMed: 8038398]

Chen LB. Mitochondrial-Membrane Potential in Living Cells. Annual Review of Cell Biology. 1988; 4:155–181.

Chen LB. Mitochondrial membrane potential in living cells. Annu Rev Cell Biol. 1988; 4:155–181. [PubMed: 3058159]

Cheng J, Cui R, Chen CH, Du J. Oxidized low-density lipoprotein stimulates p53-dependent activation of proapoptotic Bax leading to apoptosis of differentiated endothelial progenitor cells. Endocrinology. 2007; 148(5):2085–2094. [PubMed: 17289842]

Cominacini L, Pasini AF, Garbin U, Evangelista S, Crea AE, Tagliacozzi D, Nava C, Davoli A, LoCascio V. Zofenopril Inhibits the Expression of Adhesion Molecules on Endothelial Cells By Reducing Reactive Oxygen Species. American Journal of Hypertension. 2002; 15(10):891–895. [PubMed: 12372676]

Cortese JD. Rat liver GTP-binding proteins mediate changes in mitochondrial membrane potential and organelle fusion. Am J Physiol. 1999; 276(3 Pt 1):C611–620. [PubMed: 10069988]

Davidson SM, Duchen MR. Endothelial mitochondria: contributing to vascular function and disease. Circulation Research. 2007; 100(8):1128–1141. [PubMed: 17463328]

De Keulenaer GW, Chappell DC, Ishizaka N, Nerem RM, Alexander RW, Griendling KK. Oscillatory and steady laminar shear stress differentially affect human endothelial redox state: role of a superoxide-producing NADH oxidase. Circ Res. 1998; 82(10):1094–1101. [PubMed: 9622162]

de Nigris F, Franconi F, Maida I, Palumbo G, Anania V, Napoli C. Modulation by [alpha]-and [gamma]-tocopherol and oxidized low-density lipoprotein of apoptotic signaling in human coronary smooth muscle cells*. Biochemical pharmacology. 2000; 59(11):1477–1487. [PubMed: 10751558]

Deng T, Zhang L, Ge Y, Lu M, Zheng X. Redistribution of intracellular calcium and its effect on apoptosis in macrophages: Induction by oxidized LDL. Biomedicine & Pharmacotherapy. 2009; 63(4):267–274.

Dimmeler S, Haendeler J, Galle J, Zeiher AM. Oxidized low-density lipoprotein induces apoptosis of human endothelial cells by activation of CPP32-like proteases: a mechanistic clue to the 'response to injury' hypothesis. Circulation. 1997; 95(7):1760–1763. [PubMed: 9107159]

Duchen MR, Surin A, Jacobson J. Imaging mitochondrial function in intact cells. Biophotonics, Pt B. 2003; 361:353–389.

Ehrenberg B, Farkas DL, Fluhler EN, Lojewska Z, Loew LM. Membrane potential induced by external electric field pulses can be followed with a potentiometric dye. Biophysical Journal. 1987; 51(5): 833–837. [PubMed: 3593876]

Floryk D, Houstek J. Tetramethyl rhodamine methyl ester (TMRM) is suitable for cytofluorometric measurements of mitochondrial membrane potential in cells treated with digitonin. Bioscience Reports. 1999; 19(1):27–34. [PubMed: 10379904]

Forman, HJ.; Azzi, A. Production of reactive oxygen species in mitochondria and age-associated pathophysiology: a reality check. In: Cadenas, LPE., editor. Understanding the process of aging : The roles of mitochondria, Free radicals and Antioxidants. New York, Basel: Marcel Dekker Inc; 1999. p. 73-94.

Gorlach A, Brandes RP, Nguyen K, Amidi M, Dehghani F, Busse R. A gp91phox containing NADPH oxidase selectively expressed in endothelial cells is a major source of oxygen radical generation in the arterial wall. Circulation Research. 2000; 87(1):26–32. [PubMed: 10884368]

Griendling KK, FitzGerald GA. Oxidative stress and cardiovascular injury - Part II: Animal and human studies. Circulation. 2003; 108(17):2034–2040. [PubMed: 14581381]

Gutierrez J, Ballinger SW, Darley-Usmar VM, Landar A. Free radicals, mitochondria, and oxidized lipids: the emerging role in signal transduction in vascular cells. Circulation Research. 2006; 99(9):924–932. [PubMed: 17068300]

Harada-Shiba M, Kinoshita M, Kamido H, Shimokado K. Oxidized low density lipoprotein induces apoptosis in cultured human umbilical vein endothelial cells by common and unique mechanisms. Journal of Biological Chemistry. 1998; 273(16):9681–9687. [PubMed: 9545302]

Harrison D, Griendling K, Landmesser U, Hornig B, Drexler H. Role of oxidative stress in atherosclerosis. The American journal of cardiology. 2003; 91(3S):7–11.

Hausenloy DJ, Yellon DM. The mitochondrial permeability transition pore: its fundamental role in mediating cell death during ischaemia and reperfusion. Journal of Molecular and Cellular Cardiology. 2003; 35(4):339–341. [PubMed: 12689812]

Hsiai TK, Cho SK, Reddy S, Hama S, Navab M, Demer LL, Honda HM, Ho CM. Pulsatile flow regulates monocyte adhesion to oxidized lipid-induced endothelial cells. Arterioscler Thromb Vasc Biol. 2001; 21(11):1770–1776. [PubMed: 11701464]

Hsiai TK, Hwang J, Barr ML, Correa A, Hamilton R, Alavi M, Rouhanizadeh M, Cadenas E, Hazen SL. Hemodynamics influences vascular peroxynitrite formation: Implication for low-density lipoprotein apo-B-100 nitration. Free Radical Biology and Medicine. 2007; 42(4):519–529. [PubMed: 17275684]

Hwang J, Ing MH, Salazar A, Lassèque B, Griendling K, Navab M, Sevanian A, Hsiai TK. Pulsatile versus oscillatory shear stress regulates NADPH oxidase subunit expression -Implication for native LDL oxidation. Circulation Research. 2003; 93(12):1225–1232. [PubMed: 14593003]

Hwang J, Ing MH, Salazar A, Lassèque B, Griendling K, Navab M, Sevanian A, Hsiai TK. Pulsatile versus oscillatory shear stress regulates NADPH oxidase subunit expression: implication for native LDL oxidation. Circulation Research. 2003; 93(12):1225–1232. [PubMed: 14593003]

Hwang JN, Saha A, Boo YC, Sorescu GP, McNally JS, Holland SM, Dikalov S, Giddens DP, Griendling KK, Harrison DG, Jo H. Oscillatory shear stress stimulates endothelial production of O2f{ from p47phox-dependent NAD(P)H oxidases leading to monocyte adhesion. Free Radical Biology and Medicine. 2003; 35:S26–S26.

Inoue N, Ramasamy S, Fukai T, Nerem RM, Harrison DG. Shear stress modulates expression of Cu/Zn superoxide dismutase in human aortic endothelial gels. Circulation Research. 1996; 79(1):32–37. [PubMed: 8925565]

Korshunov SS, Skulachev VP, Starkov AA. High protonic potential actuates a mechanism of production of reactive oxygen species in mitochondria. FEBS Letters. 1997; 416(1):15–18. [PubMed: 9369223]

Ku DN, Giddens DP, Zarins CK, Glagov S. Pulsatile flow and atherosclerosis in the human carotid bifurcation. Positive correlation between plaque location and low oscillating shear stress. Arteriosclerosis. 1985; 5(3):293–302. [PubMed: 3994585]

Kudo S, Morigaki R, Saito J, Ikeda M, Oka K, Tanishita K. Shear-stress effect on mitochondrial membrane potential and albumin uptake in cultured endothelial cells. Biochemical and Biophysical Research Communications. 2000; 270(2):616–621. [PubMed: 10753672]

Lee I, Bender E, Kadenbach B. Control of mitochondrial membrane potential and ROS formation by reversible phosphorylation of cytochrome c oxidase. Molecular and Cellular Biochemistry. 2002; 234(1):63–70. [PubMed: 12162461]

Li HL, Wang AB, Zhang R, Wei YS, Chen HZ, She ZG, Huang Y, Liu DP, Liang CC. A20 inhibits oxidized low-density lipoprotein-induced apoptosis through negative Fas/Fas ligand-dependent activation of caspase-8 and mitochondrial pathways in murine RAW264. 7 macrophages. Journal of cellular physiology. 2006; 208(2):307–318. [PubMed: 16646083]

Li R, Beebe T, Cui J, Rouhanizadeh M, Ai L, Wang P, Gundersen M, Takabe W, Hsiai TK. Pulsatile shear stress increased mitochondrial membrane potential: Implication of Mn-SOD. Biochemical and Biophysical Research Communications. 2009; 388(2):406–412. [PubMed: 19666009]

Liberman EA, Topaly VP, Tsofina LM, Jasaitis AA, Skulachev VP. Mechanism of Coupling of Oxidative Phosphorylation and Membrane Potential of Mitochondria. Nature. 1969; 222(5198):1076. [PubMed: 5787094]

Liu X, Zhao J, Xu J, Zhao B, Zhang Y, Zhang S, Miao J. Protective effects of a benzoxazine derivative against oxidized LDL-induced apoptosis and the increases of integrin [beta] 4, ROS, NF-[kappa] B and P53 in human umbilical vein endothelial cells. Bioorganic & Medicinal Chemistry Letters. 2009; 19(10):2896–2900. [PubMed: 19362839]

Loew LM, Tuft RA, Carrington W, Fay FS. Imaging in five dimensions: time-dependent membrane potentials in individual mitochondria. Biophysical Journal. 1993; 65(6):2396–2407. [PubMed: 8312478]

Martinet W, Kockx MM. Apoptosis in atherosclerosis: focus on oxidized lipids and inflammation. Current opinion in lipidology. 2001; 12(5):535–541. [PubMed: 11561173]

Mitchell JW, Thomas JA. Role of ATP in Phosphorylation of Bovine Heart Glycogen Synthase. Federation Proceedings. 1979; 38(3):480–480.

Navab M, Berliner JA, Watson AD, Hama SY, Territo MC, Lusis AJ, Shih DM, Van Lenten BJ, Frank JS, Demer LL, Edwardsm PA, Fogelman AM. The Yin and Yang of oxidation in the development of the fatty streak. A review based on the 1994 George Lyman Duff Memorial Lecture. Arteriosclerosis, Thrombosis, and Vascular Biology. 1996; 16(7):831–842.

Nicholls DG. Simultaneous monitoring of ionophore- and inhibitor-mediated plasma and mitochondrial membrane potential changes in cultured neurons. Journal of Biological Chemistry. 2006; 281(21):14864–14874. [PubMed: 16551630]

Nisoli E, Clementi E, Carruba MO, Moncada S. Defective mitochondrial biogenesis - A hallmark of the high cardiovascular risk in the metabolic syndrome? Circulation Research. 2007; 100(6):795–806. [PubMed: 17395885]

Robinson KM, Janes MS, Pehar M, Monette JS, Ross MF, Hagen TM, Murphy MP, Beckman JS. Selective fluorescent imaging of superoxide in vivo using ethidium-based probes. Proceedings of the National Academy of Sciences of the United States of America. 2006; 103(41):15038–15043. [PubMed: 17015830]

Robinson KM, Janes MS, Pehar M, Monette JS, Ross MF, Hagen TM, Murphy MP, Beckman JS. Selective fluorescent imaging of superoxide in vivo using ethidium-based probes. Proc Natl Acad Sci U S A. 2006; 103(41):15038–15043. [PubMed: 17015830]

Scaduto RC, Grotyohann LW. Measurement of mitochondrial membrane potential using fluorescent rhodamine derivatives. Biophysical Journal. 1999; 76(1):469–477. [PubMed: 9876159]

Senior AE. ATP Synthesis by Oxidative-Phosphorylation. Physiological Reviews. 1988; 68(1):177–231. [PubMed: 2892214]

Sorescu GP, Song H, Tressel SL, Hwang J, Dikalov S, Smith DA, Boyd NL, Platt MO, Lassèque B, Griendling KK, Jo H. Bone morphogenic protein 4 produced in endothelial cells by oscillatory shear stress induces monocyte adhesion by stimulating reactive oxygen species production from a nox1-based NADPH oxidase. Circ Res. 2004; 95(8):773–779. [PubMed: 15388638]

Stocker R, Keaney JF Jr. Role of oxidative modifications in atherosclerosis. Physiological Reviews. 2004; 84(4):1381–1478. [PubMed: 15383655]

Storz P. Mitochondrial ROS - radical detoxification, mediated by protein kinase D. Trends in Cell Biology. 2007; 17(1):13–18. [PubMed: 17126550]

Ward MW, Rego AC, Frenquelli BG, Nicholls DG. Mitochondrial membrane potential and glutamate excitotoxicity in cultured cerebellar granule cells. Journal of Neuroscience. 2000; 20(19):7208–7219. [PubMed: 11007877]

Zmijewski JW, Moellering DR, Le Goffe C, Landar A, Ramachandran A, Darley-Usmar VM. Oxidized LDL induces mitochondrially associated reactive oxygen/nitrogen species formation in endothelial cells. American Journal of Physiology- Heart and Circulatory Physiology. 2005; 289(2):H852–861. [PubMed: 15805232]

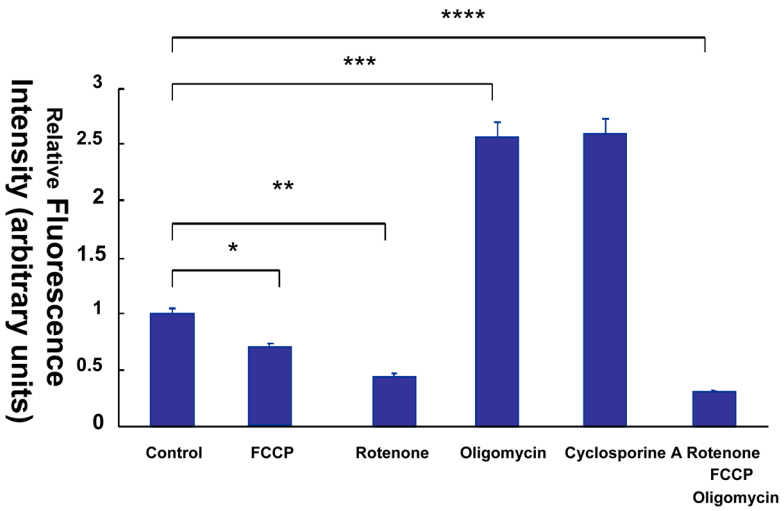


**Fig. 9.36.1.**

Mitochondrial membrane potential ($\Delta\Psi_m$) in response to mitochondrial respiratory chain inhibitors and uncouplers in endothelial cells. (a) Flow cytometry analysis was performed to monitor the $TMRM^+$-stained HAEC. In the presence of FCCP and rotenone, the $TMRM^+$ intensity was decreased by 25% and 55%, respectively, in comparison with the control (*,** $P < 0.05$, n = 5). In the presence of oligomycin and Cyclosporine-A, the $TMRM^+$ intensity was increased by about 2.5-fold (*** $P < 0.05$). Treatment with a combination of FCCP, oligomycin and rotenone decreased $TMRM^+$ intensity by 71% (****$P < 0.05$, n = 5). **(b)** Nernst equation was applied to convert TMRM+ signals to $\Delta\Psi_m$. The changes in $\Delta\Psi_m$ in response to mitochondrial respiratory chain inhibitors and uncouplers followed the trends in $TMRM^+$ intensity.

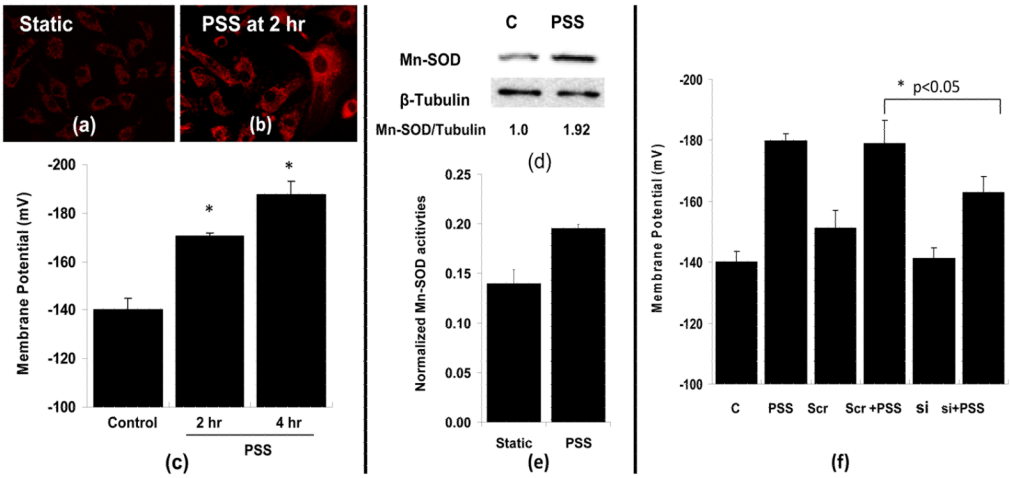


**Fig. 9.36.2.**

Pulsatile shear stress increases mitochondrial membrane potential by up-regulating Mn-SOD activities. **(a)** & **(b)** PSS exposure for 2 hours increases $TMRM^+$ cationic dye intensity for $\Delta\Psi_m$ in HAEC compared to the static condition. **(c)** $TMRM^+$ intensity was measured by FACS and calibrated to voltage (mV) for $\Delta\Psi_{m.}$ (* $p < 0.05$ versus static condition, n = 4) (**d**) PSS exposure for 4 hours increased Mn-SOD protein expression normalized to β-tubulin. **(e)** Mn-SOD activities were also up-regulated in response to PSS. **(f)** HAEC were transfected with control siRNA (Scr) or siMn-SOD (si), followed by exposure to shear stress or static condition. siMn-SOD attenuated PSS induced $\Delta\Psi_m$ as compared to control siRNA (* $p<$ 0.05, n = 3).

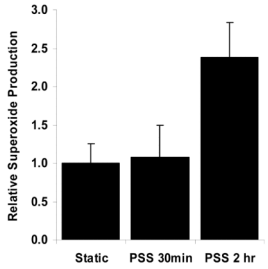


**Fig. 9.36.3.**

HAECs were exposed to PSS for 30 minutes or 2 hours. Mitochondrial superoxide production was measured by flow cytometry using mitochondrial superoxide probe MitoSOX Red. Relative superoxide production was calculated based on fluorescence intensity.

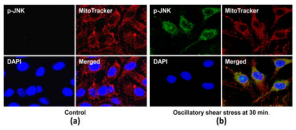


**Fig. 9.36.4.**

JNK Activation in Response to OSS. **(a)** p-JNK was stained with FITC-anti-p-JNK (green). Active cellular mitochondria were localized using MitoTracker Red. Nuclei were stained with DAPI (blue). Under static conditions, JNK green fluorescence was hardly visible. **(b)** In response to OSS, a significant JNK green fluorescence developed after 30 minutes, accompanied with yellowish/orange signals as a result of merged spectra between FITC and MitoTracker Red.

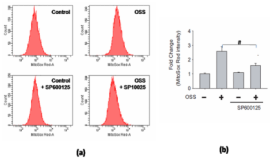


**Fig. 9.36.5.**

Inhibition of JNK attenuated MitoSOX Red intensities. BAEC monolayers were pre-treated with JNK inhibitor, SP600125, and mitochondrial $O_2^{\cdot -}$ specific dye, Mitosox Red, prior to flow exposure. Measurements were performed in duplicates using BD LSR II flow cytometer. **(a)** The data were presented by histograms in terms of the mean intensity of MitoSOX fluorescence normalized to those of the static conditions. **(b)** OSS-induced MitoSOX intensity was significantly attenuated in response to JNK inhibitor ($^{\#}P < 0.01$, n=3).

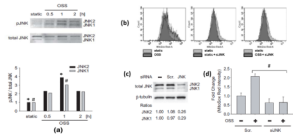

**Fig. 9.36.6.**

Oscillatory shear stress increased MitoSOX Red intensities via JNK activation. **(a)** BAEC monolayers were exposed to static condition versus oscillatory shear stress (OSS) for 30 minutes, 1 hour, or 2 hours. Phosphorylated JNK was expressed as fold ratios relative to total JNK and static conditions. OSS induced a peaked JNK activation at 1 hour (both JNK isoforms) (*$P$ < 0.01, n=3). **(b)** Flow cytometry analyses of the mean intensities of MitoSOX fluorescence normalized to the static controls in response to OSS, static + siJNK, and OSS + siJNK. **(c)** Small interfering JNK-1 and JNK-2 (siJNK) significantly knocked down JNK from 2.1- to 0.65-fold as compared to the control and scrambled JNK (Scr). **(d)** The histograms showed that transfecting siJNK significantly reduced OSS-mediated MitoSOX intensity ($^{\#}P$ < 0.01, n=3)

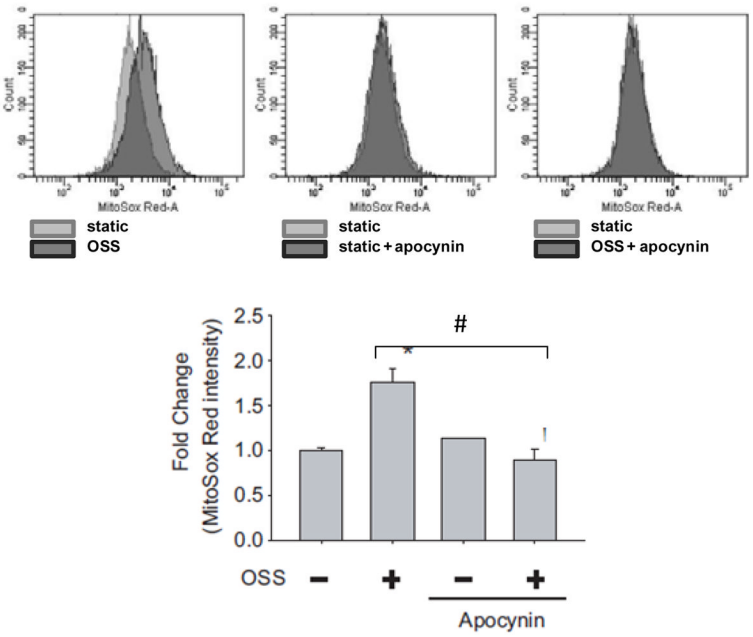


**Fig. 9.36.7.**

Inhibition of NADPH oxidase attenuated OSS-induced MitoSOX intensities. MitoSOX fluorescence was measured by flow cytometer. (a) The data were presented by histograms in terms of the mean intensity of MitoSOX fluorescence normalized to those of the static controls. (b) While OSS induced an increase in MitoSOX fluorescence by 1.75±0.2 (*$P$ < 0.01 versus static conditions, n=3), pre-treatment with Apocynin significantly attenuated OSS-induced MitoSOX intensity ($^{\#}P$ < 0.01, n=3).

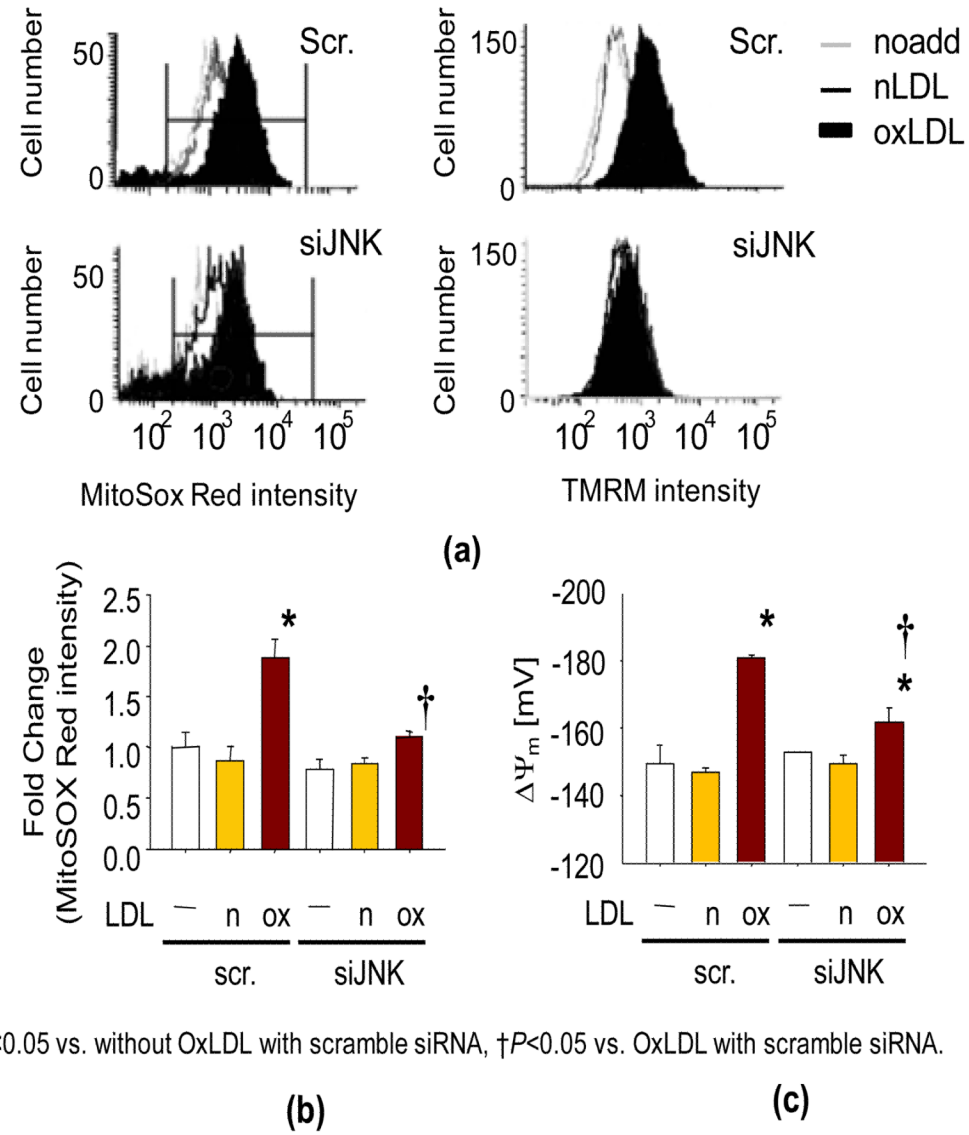


*$P$<0.05 vs. without OxLDL with scramble siRNA, †$P$<0.05 vs. OxLDL with scramble siRNA.

**Fig. 9.36.8.**

SiJNK attenuated OxLDL-induced mitochondrial redox status. HAEC were transfected with siJNK or scramble siRNA for 48 hours. (a) Cell lysate was used to verify the efficiency of siJNK on the protein level of JNK. (b) Cells were pre-incubated with 5μmol/L of MitoSox Red for 10 minutes at 37°C. Next, cells were cultured in the absence or presence of 50μg/mL of OxLDL for 1 hour. Cells were fixed by 1% PFA and fluorescent intensity was measured by FACS. Left, typical histograms were showed in the absence and presence of LDLs (Top: scr siRNA, bottom: siJNK). Right, bar-graph was quantified from gated area shown in the histograms. *$P$<0.05 vs. in the absence of OxLDL and in the presence of scramble siRNA (lane 1), †$P$<0.05 vs. in the presence of OxLDL and in the presence of scramble siRNA (lane 3). (c) Cells were exposed to 50μg/mL of OxLDL for 1 hour and $TMRM^+$ intensity was measured by FACS. The fluorescence intensity was converted to mitochondrial membrane polarization ($\Delta\Psi_m$) as described in the background information section *$P$<0.05 vs. in the absence of OxLDL and in the presence of scramble siRNA (lane 1), †$P$<0.05 vs. in the presence of OxLDL and in the presence of scramble siRNA (lane 3).

These data represented the means from triplicates of two independent experiments. Scr. denoted scramble; n native LDL; and ox OxLDL.

**Table 9.36.1**

List of problems and suggested solutions.

| Potential Problem | Possible Reason | Suggested Solution |
|---|---|---|
| High Background | • Cells metabolically too active<br>• Fluorescence dye concentration too high<br>• Incubation time too long<br>• Cell death and aggregation | • Starve cells for 4 hours or over night<br>• Reduce and optimize fluorescence dye amount<br>• Reduce incubation time<br>• Avoid damaging cells and optimize dissociation of cells |
| Low signal | • Dye leaching out of cells<br>• Not optimized dye concentration, incubation time or reagent degradation<br>• Bleaching of signals | • Analyze sample immediately<br>• Use positive and negative control to optimize conditions<br>• Avoid exposure to light |
| No difference in fluorescence | • Not optimized conditions<br>• Reagent disrupt membrane potential and subsequent specific dye uptake<br>• Superoxide reaction with NO to form peroxynitrite | • See above to control background and optimize dye concentration and incubation time<br>• Control cell culture condition to ensure cell health status and no membrane potential disruptors.<br>• Use pan-NO synthesis inhibitor |

**Table 9.36.2**

$\Delta\Psi_m$ in response to electron transport chain inhibitors and uncouplers.

| | ΔΨm (mean) | ± STD |
|---|---|---|
| **Control** | −140.00 | 6.89 |
| **FCCP** | −118.64 | 4.98 |
| **Rotenone** | −107.81 | 7.34 |
| **Oligomycine** | −165.01 | 4.23 |
| **Cyclosporine A** | −165.29 | 9.80 |
| **rotenone/FCCP/Oligomycin** | −88.00 | 3.90 |